DOI 10.5162/sensor2017/A4.2

Detection of short trace gas pulses

Tobias Baur[1], Andreas Schütze[1], Tilman Sauerwald[1]
[1] Saarland University, Laboratory for Measurement Technology, Campus A5 1, 66123 Saarbrücken, Germany
t.baur@lmt.uni-saarland.de

Abstract
A novel method for detection of short gas pulses at very low concentrations is presented. The approach is based on a special temperature modulation technique leading to the differential measurement of surface reduction (DSR) of a metal oxide semiconductor (MOS) gas sensor. For this method, the sensor surface is oxidized at high temperature (e.g. 400 °C). An abrupt step in temperature to e.g. 100 °C results in a nonequilibrium state with a strong excess of negative surface charges. Reactions of these surface charges with reducing gas are prevailing and lead to a very high sensitivity. Applying the method to a commercial SnO_2 sensor, gas pulses down to 1 ppb·s (ppb times seconds) can be detected as demonstrated for ethanol.

Key words: MOS gas sensor, differential surface reduction (DSR), short gas pulses.

Motivation

The measurement of short gas pulses is essential in analytical gas sensing microsystems, e.g., integrated sensor-pre-concentrator systems [1] and micro gas chromatographs (µGC) [2]. While some progress has been reported in the miniaturization of GC columns [2, 3] miniature detectors with a low detection limit are still required. MOS sensors are ideal due to their small size [2]. Moreover, recent results show that the sensitivity of MOS sensors can be enhanced significantly by a special operation mode.

Differential surface reduction

We use the differential surface reduction (DSR) method to measure short gas pulses. DSR is derived from a model for semiconductor gas sensors under temperature modulation presented in our earlier work [4, 5]. This model is based on a simplified single grain to grain contact [6]. A depletion zone is formed by binding electrons to ionosorbed oxygen. Conduction electrons have to overcome the resulting energy barrier E_b. The conductance of the sensor can be described by Eq. (1) showing the exponential dependence of the conductance from E_b with the Boltzmann constant k_b, the temperature T of the sensor film and a prefactor G_0.

$$G = G_0 \cdot e^{-\frac{E_b}{k_b T}} \quad (1)$$

The principle of gas sensing with metal oxide semiconductor gas sensors is based on oxidation and reduction on the surface. It causes an exchange of electrons between conduction band and surface states. Thereby, the energy barrier E_b is changed. In clean dry air, the surface will be oxidized primarily by ionosorbed oxygen [6]. Reducing gas molecules react with ionosorbed oxygen and the oxygen molecules release their electron into the conduction band. The oxidation and reduction of the surface can be influenced by temperature. In TCO (temperature cycled operation) the sensor temperature is changed periodically typically with a cycle period of some seconds up to a few minutes. On this timescale, the sensor is driven to different nonequilibrium states. The relaxation to the temperature dependent equilibrium is influenced by reaction with reducing or oxidizing gases and the oxidation with ambient oxygen. Fig. 1 shows the schematic Arrhenius plot for instantaneous sensor heating and cooling and the relaxation of the conductance on long hot and cold temperature plateaus, respectively. It includes a sketch of the grain to grain boundary for different points of the temperature cycle.

In equilibrium state 1 at low temperature, the sensor has a small negative surface charge. A fast rise from low to high temperature (1 to 2) causes a conductance rise of the sensor. Due to the fast temperature change the surface occupation remains nearly constant. During

relaxation at high temperature a decrease in conduction caused by oxidation of the surface is observed (2 to 3). Abruptly cooling down to a low temperature (3 to 4) causes a strong excess of negative surface charge, because of the unchanged high surface occupation stemming from the high temperature equilibrium. In this low temperature phase reactions with reducing gases are strongly favored over additional oxidation of the surface. For a short duration, the derivative of the logarithmic conductance ln(G) is proportional to the time-dependent rate constant k of surface reduction by reducing gas (Eq. (2)) [5].

$$\frac{d \ln G}{dt} \sim k(t) \sim c(t) \qquad (2)$$

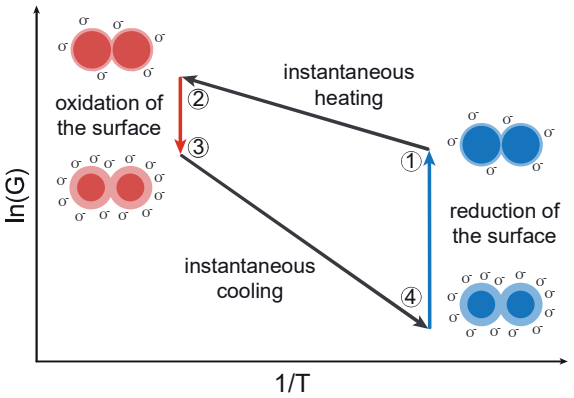

Fig. 1. Schematic Arrhenius plot of a MOS-sensor during TCO with sketches depicting the grain-grain boundary in different states.

For low concentrations, the rate constant is proportional to the concentration [4, 5]. Therefore, the measurement of the differential reduction of the surface in this phase especially at very low temperature (e.g. 100 °C) allows a very sensitive detection of short gas pulses and the quantification of the peak area.

$$\ln G(t_2) - \ln G(t_1) \sim \int_{t_1}^{t_2} c(t) \qquad (3)$$

Fig. 2 shows the schematic conductance curve with a temperature jump from low to high temperature at t = 0 followed by relaxation at high temperature and subsequent temperature jump to low temperature. During the low temperature stage one concentration peak ($c \cdot \Delta t$) is assumed.

Measurement

Measurements were performed using a commercial SnO_2 sensor (AS-MLV, ams Sensor Solutions Germany GmbH). The sensor is specified for VOC detection (e.g. for indoor air quality) and the manufacturer recommends an operating temperature of 320 °C with a baseline resistance of 100 (10) to 500 kΩ (2 µS) [7]. In earlier work, we showed that for this particular sensor the sensitivity can be increased by many orders of magnitude with temperature cycled operation [4]. Along with the increase of sensitivity the range of sensor resistance is increased by several orders of magnitude reaching minimum conductance values below 10 pS.

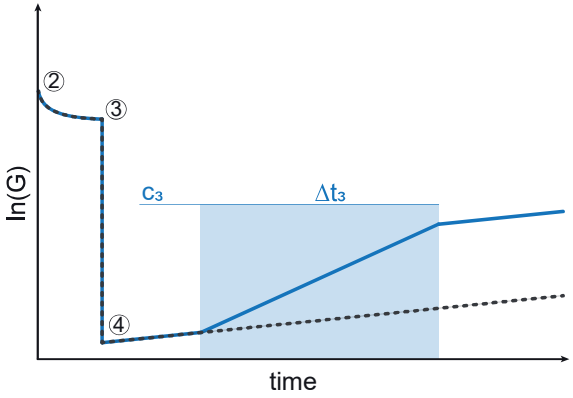

Fig. 2. Schematic conductance curve for DSR with a temperature jump from high to low temperature; during the relaxation at the low temperature stage, one concentration peak is assumed.

For the validation of the DSR approach, we use a temperature cycle with two temperature plateaus, an oxidation phase at 400 °C with a duration of 60 s and a reduction phase at 100 °C with a duration of 600 s. The temperature of the sensor is controlled via the heater resistance by a digital PID (proportional–integral–derivative) controller with a resolution of 0.1 °C. The time constant τ_{63} for cooling down of the sensor (450 °C to 150 °C) is below 7 ms [5]. For the temperature modulations used in this investigation the AS-MLV has a large dynamic range from 100 µS down to 2.5 pS. Semiconductor sensors must be measured with a low constant voltage (typically few 100 mV) to prevent influences from Joule heating and of electromigration throughout the measurement. The resulting current through the sensor is usually measured using a reference resistor. At a low sensor conductance, the voltage drop over the reference resistor is very small. The resolution and noise of the voltage measurement is therefore limiting the measurement range at low conductance.

The aim of the DSR method is the measurement of the rate constant for the change of the surface charge which is proportional to the logarithmic conductance. Thus, a low relative error at low conductance combined with a high sample rate is prerequisite for a low detection limit. In our approach, we measure the resulting current with a logarithmic amplifier (log amp). An error

in the conductance measurement is contributing linearly to the error for the rate constant.

$$\log G \pm \Delta \log G = k_d \pm \Delta k_d \qquad (4)$$

We chose a LOG114 amplifier (Texas Instruments Inc.). To achieve reliable measurements at very low conductance values, the voltage is increased to 4 V across the sensor. To limit the influence of Joule heating across the sensor and to protect it at low sensor resistance, a 100 kΩ resistor is connected in series with the sensor. According to the datasheet the LOG114 has a dynamic range from 100 pA to 10 mA [8]. We tested several LOG114 chips with a constant voltage supply from a Keithley Sourcemeter 2602b and reference resistors from 10 kΩ up to 10 GΩ. We observed that even smaller currents could be measured by these devices. Most of the tested log amps could measure down to 10 pA and some even down to 1 pA with good agreement to the reference sourcemeter. Thus, the developed sensor read-out circuit covers a resistance range over 11 orders of magnitude, e.g. from 250 µS down to 2.5 pS, with a fast sample rate of 2 kHz.

We tested the effective resolution of the log amp system with a test setup, i.e. the smallest variation on the sensor current that can be detected reliably by the sensor. A voltage of 0.5 V is applied from a filtered linear voltage regulator across the reference resistors (100 Ω to 10 GΩ). The output voltage of the log amp is measured with the reference sourcemeter at 5 kS/s (50,000 points). The reference resistors had wire leads and an accuracy of 1 %. The whole test setup was placed in a shielded housing. Fig. 3 shows the effective resolution of the log amp dependent on the current.

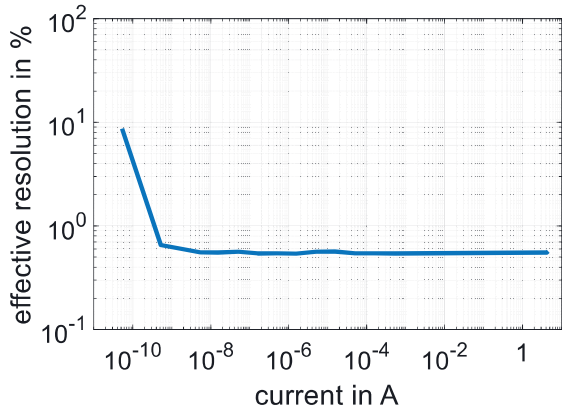

Fig. 3. Effective resolution at 5 kS/s of the log amp tested with reference resistors; measurement conditions: 0.5 V across the reference resistor, log out voltage measured with Keithley Sourcemeter 2602b at 5 kHz sample rate.

In the measurement range between 10 mA and 500 pA the error is almost constant at 0.6 %. This indicates that the error is dominated from noise in the voltage measurement setup at the log amp output. For current values below 500 pA the error is strongly depending on the current presumably it is dominated by noise in the input current. One reason for this electromagnetic noise can be the wire leads of our reference resistors. The gas sensor has much shorter leads. As a consequence, we achieve lower noise (compare Fig. 6) than with the reference resistor.

The gas measurements were realized with our gas mixing system (GMA) based on gas pre-dilution to achieve very low concentrations and a large concentration range [9]. The current set-up comprises four pre-dilution lines for the generation of trace gases with a dynamic concentration range c_{bottle}/c_{set} from 5 to 312,750. Here, c_{set} is the set concentration and c_{bottle} is the concentration in the test gas bottle. Dry zero air with a flow of 100 ml/min is used as carrier gas. The zero air is generated by a two-step purification process. The first step is a charcoal filter system which removes hydrocarbons (larger than C_3) very efficiently also removes humidity and CO_2 with a pressure swing. The second step is based on a catalytic conversion to remove the smaller hydrocarbons as well as hydrogen and carbon monoxide. Ethanol as test gas was supplied by a gas cylinder with 200 ppm in synthetic air 4.6 and subsequent dilution in zero air. The mixing ratio of the pre-dilution was allowed to stabilize for several minutes before measurements. Gas pulses were created by switching a solenoid valve. To achieve gas pulses with a short duration the sensor is placed in an optimized sensor chamber with low dead volumes and optimized gas transport to the sensor. Fig. 4 shows a CAD drawing and Fig. 5 shows a cross section of the sensor chamber.

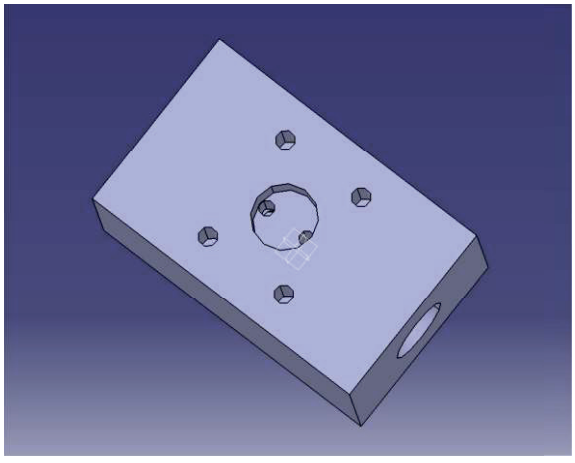

Fig. 4. CAD model of the sensor chamber.

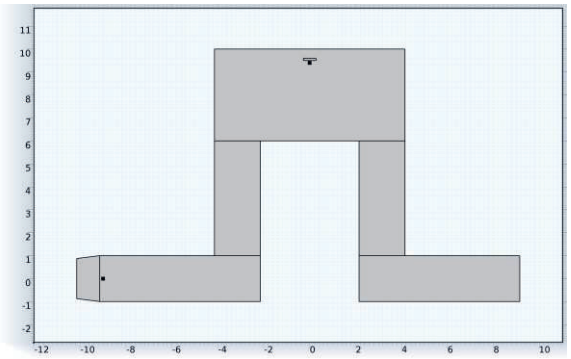

Fig. 5. Cross section of the CAD drawing of the sensor chamber. The microsensor in placed at the top.

Results and conclusion

Fig. 6 shows the result proving the DSR functional principle with an ethanol pulse of 10 ppb·s (5 ppb for 2 s). For two DSR measurements (at 100 °C) the time-dependent conductance is shown with (blue solid line) and without ethanol (blue dotted line) peak. Obviously, the reproducibility of the measurements is very high as the solid and the dotted line are matching almost perfectly up to the injection of ethanol. The measurement without ethanol is used as background and the constant slope of this background $k_{d,air}$ was subtracted from the measurement curve. The time-dependent rate constant $k_{d,gas}$ (orange line) is derived from the derivative of the measurement curve (Eq. (5)) [5].

$$k_{d,gas} = \frac{k_b T}{2E_b(t_0)} \frac{d \ln G}{dt} - k_{d,air} \qquad (5)$$

Here, $E_b(t_0)$ is the energy barrier at time t_0 when the temperature changes. $E_b(t_0)$ can be calculated from the conductance difference from high to low temperature [5]. We use a cubic smooth spline and a Savitzky–Golay filter with 1000 points (500 ms) to reduce the noise in the conductance measurement and to improve the numerical differentiation of the signal. The prediction of the sensor model (Eq. (2)) is very good. Furthermore, the reproducible detection of the same amount of substance by different combinations of pulse duration and concentration was tested. Tab. 1 shows the results of the integrated rate constants for pulses with 100 and 1000 ppb·s of ethanol. Here, good agreement of gas pulses with the same total amount is observed as predicted by Eq. (3).

We have successfully demonstrated that a sensor operated in DSR mode is capable of detecting short pulses of reducing gas at very low concentrations. This opens the way for small and inexpensive microsystems for the detection of trace gases using a sensor pre-concentrator system.

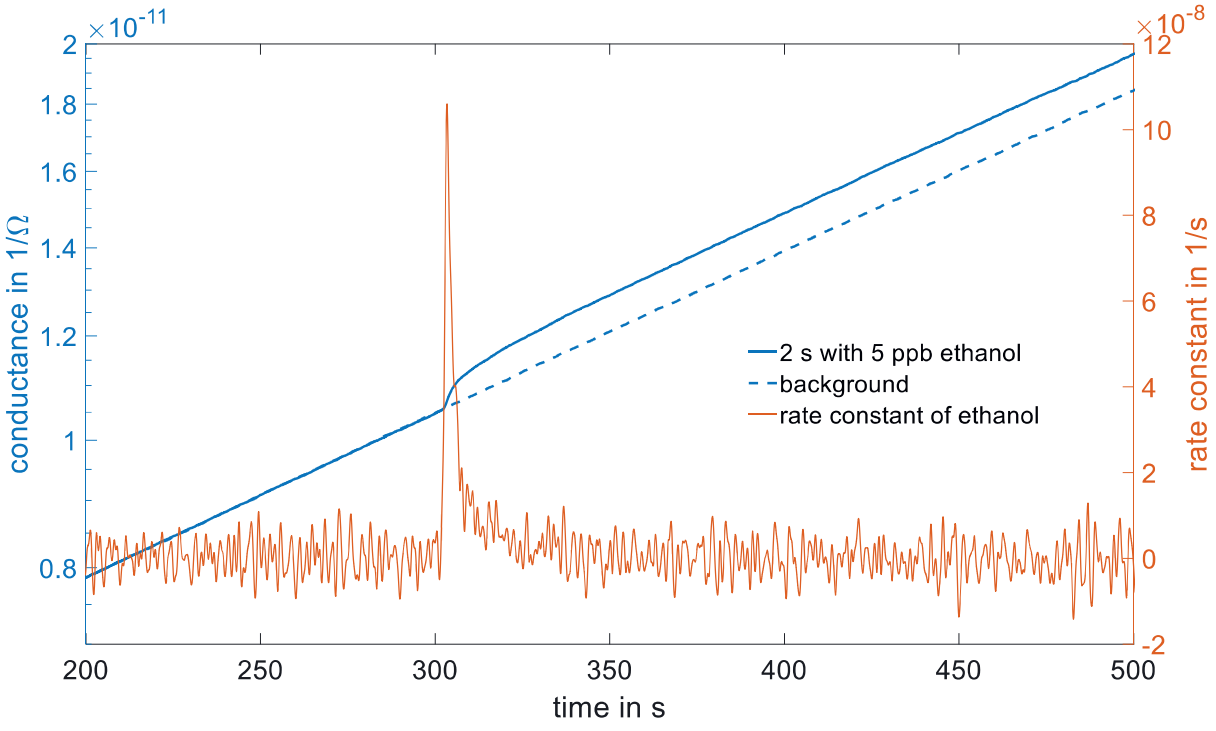

Fig.6. Blue: time-dependent conductance during 100 °C phase without (dotted) and with (solid) 10 ppb·s ethanol pulse. Orange: time-dependent rate constant of ethanol.

Tab. 1: Peak areas for different duration and concentration combinations with the same amount of substance.

amount of substance (ppb·s)	duration (s)	concentration (ppb)	integrated rate constant (a.u.)
10	1	10	0.00136
10	5	2	0.00142
100	1	100	0.0122
100	5	20	0.0120

References

[1] M. Leidinger, M. Rieger, T. Sauerwald, C. Alépée, A. Schütze, Integrated pre-concentrator gas sensor microsystem for ppb level benzene detection, *Sensors and Actuators B: Chemical* 236, 988-996 (2016); doi: 10.1016/j.snb.2016.04.064

[2] S. Zampolli, I. Elmi, F. Mancarella, P. Betti, E. Dalcanale, G.C. Cardinali, M. Severi, Real-time monitoring of sub-ppb concentrations of aromatic volatiles with a MEMS-enabled miniaturized gas-chromatograph, *Sensors and Actuators B: Chemical* 141, 322–328 (2009); doi: 10.1016/j.snb.2009.06.021

[3] M. Akbar, H. Shakeel, M. Agah, F.L. Dorman, J.J. Whiting, J.W. Cochran, J. Gardea-Torresdey, A. Boots, GC-on-chip: integrated column and photoionization detector, *Lab Chip* 15, The Royal Society of Chemistry, 1748–1758 (2015); doi: 10.1039/C4LC01461H

[4] T. Baur, A. Schütze, T. Sauerwald, Optimierung des temperaturzyklischen Betriebs von Halbleitergassensoren, *tm - Technisches Messen,* 82, 187–195 (2015); doi: 10.1515/teme-2014-0007

[5] C. Schultealbert, T. Baur, A. Schütze, S. Böttcher, T. Sauerwald, A novel approach towards calibrated measurement of trace gases using metal oxide semiconductor sensors, *Sensors & Actuators: B. Chemical* 239, 390–396 (2017); doi: 10.1016/j.snb.2016.08.002

[6] J. Ding, T. McAvoy, R. Cavicchi, E. Richard, S. Semancik, Surface state trapping models for SnO2-based microhotplate sensors, *Sensors and Actuators B: Chemical* 77, 597–613 (2001); doi: 10.1016/S0925-4005(01)00765-1

[7] Applied Sensors GmbH, VOC Sensor - AS-MLV Datasheet (2013).

[8] Texas Intruments Inc., LOG114 - Logarithmic Amplifier Datasheet (2007).

[9] N. Helwig, M. Schüler, C. Bur, A. Schütze, T. Sauerwald, Gas mixing apparatus for automated gas sensor characterization, *Measurement Science and Technology* 25 (2014); doi: 10.1088/0957-0233/25/5/055903